Available online at www.sciencedirect.com
ScienceDirect
Nuclear Instruments and Methods in Physics Research A 591 (2008) 490–509
NUCLEAR INSTRUMENTS & METHODS IN PHYSICS RESEARCH Section A
www.elsevier.com/locate/nima

Systematic study of trace radioactive impurities in candidate construction materials for EXO-200

D.S. Leonard[a,*], P. Grinberg[b], P. Weber[c,1], E. Baussan[c,2], Z. Djurcic[a,3], G. Keefer[a], A. Piepke[a], A. Pocar[d], J.-L. Vuilleumier[c], J.-M. Vuilleumier[c], D. Akimov[e], A. Bellerive[f], M. Bowcock[f], M. Breidenbach[g], A. Burenkov[e], R. Conley[g], W. Craddock[g], M. Danilov[e], R. DeVoe[d], M. Dixit[f], A. Dolgolenko[e], I. Ekchtout[f], W. Fairbank Jr. [h], J. Farine[i], P. Fierlinger[d], B. Flatt[d], G. Gratta[d], M. Green[d], C. Hall[j], K. Hall[h], D. Hallman[i], C. Hargrove[f], R. Herbst[g], J. Hodgson[g], S. Jeng[h], S. Kolkowitz[d], A. Kovalenko[e], D. Kovalenko[e], F. LePort[d], D. Mackay[g], M. Moe[k], M. Montero Díez[d], R. Neilson[d], A. Odian[g], K. O'Sullivan[d], L. Ounalli[c], C.Y. Prescott[g], P.C. Rowson[g], D. Schenker[c], D. Sinclair[f], K. Skarpaas[g], G. Smirnov[e], V. Stekhanov[e], V. Strickland[f], C. Virtue[i], K. Wamba[g], J. Wodin[d,4]

[a]*Department of Physics and Astronomy, University of Alabama, Tuscaloosa, AL, USA*
[b]*Institute for National Measurements Standards, National Research Council Canada, Ottawa, ON, Canada*
[c]*Institut de Physique, Université de Neuchatel, Neuchatel, Switzerland*
[d]*Physics Department, Stanford University, Stanford, CA, USA*
[e]*ITEP, Moscow, Russia*
[f]*Physics Department, Carleton University, Ottawa, ON, Canada*
[g]*Stanford Linear Accelerator Center, Menlo Park, CA, USA*
[h]*Physics Department, Colorado State University, Fort Collins, CO, USA*
[i]*Department of Physics, Laurentian University, Sudbury, ON, Canada*
[j]*Department of Physics, University of Maryland, College Park, MD, USA*
[k]*Physics Department, University of California, Irvine, CA, USA*

Received 1 October 2007; received in revised form 25 February 2008; accepted 4 March 2008
Available online 18 March 2008

Abstract

The Enriched Xenon Observatory (EXO) will search for double beta decays of ^{136}Xe. We report the results of a systematic study of trace concentrations of radioactive impurities in a wide range of raw materials and finished parts considered for use in the construction of EXO-200, the first stage of the EXO experimental program. Analysis techniques employed, and described here, include direct gamma counting, alpha counting, neutron activation analysis, and high-sensitivity mass spectrometry.

PACS: 82.80.Jp; 14.60.Pq; 23.40.−s; 23.40.Bw

Keywords: Radiopurity; Trace analysis; Neutron activation analysis; Mass spectrometry; Mass spectroscopy; Germanium counting; Alpha counting; Low background; Double beta decay; EXO; EXO-200

*Corresponding author. Tel.: +1 205 348 6066; fax: +1 205 348 5051.
E-mail address: dleonard@bama.ua.edu (D.S. Leonard).
[1]Now at Center for Ion Beam Physics, Swiss Universities for Applied Physics, La Chaux-de-Fonds, Switzerland.
[2]Now at IPHC, Université Louis Pasteur, CNRS/IN2P3, Strasbourg, France.
[3]Now at Columbia University, NewYork, NY, USA.
[4]Now at Stanford Linear Accelerator Center, Menlo Park, CA, USA.

0168-9002/$ - see front matter © 2008 Elsevier B.V. All rights reserved.
doi:10.1016/j.nima.2008.03.001

1. Introduction

This work was motivated by the Enriched Xenon Observatory (EXO), a multi-stage experimental research program with the purpose of detecting rare double beta decays in ^{136}Xe [1]. With EXO-200, the first stage of the project, we will search for these decays in an underground cryogenic time-projection chamber (TPC) filled with approximately 200 kg of liquid xenon enriched to 80% in ^{136}Xe. The EXO-200 detector is shown in Fig. 1 and described in more detail in Ref. [2]. To reach the desired half-life sensitivity of about 6×10^{25} yr for the 0-neutrino decay mode, the background rate of candidate events (single-site events within 2-σ of the Q value of 2458 keV [3]) cannot exceed about 20 events per year. The background rate for the 2-neutrino decay mode should not exceed about 30 000 events per year between a threshold of approximately 400 keV and the Q value. Similarly strict background requirements are common to other double beta decay and rare-event detectors. To achieve very low background rates, all materials present in the detector, and even some external materials that are in the path of the xenon circulation or the cryogenic fluid handling, must be selected to have very low intrinsic concentrations of

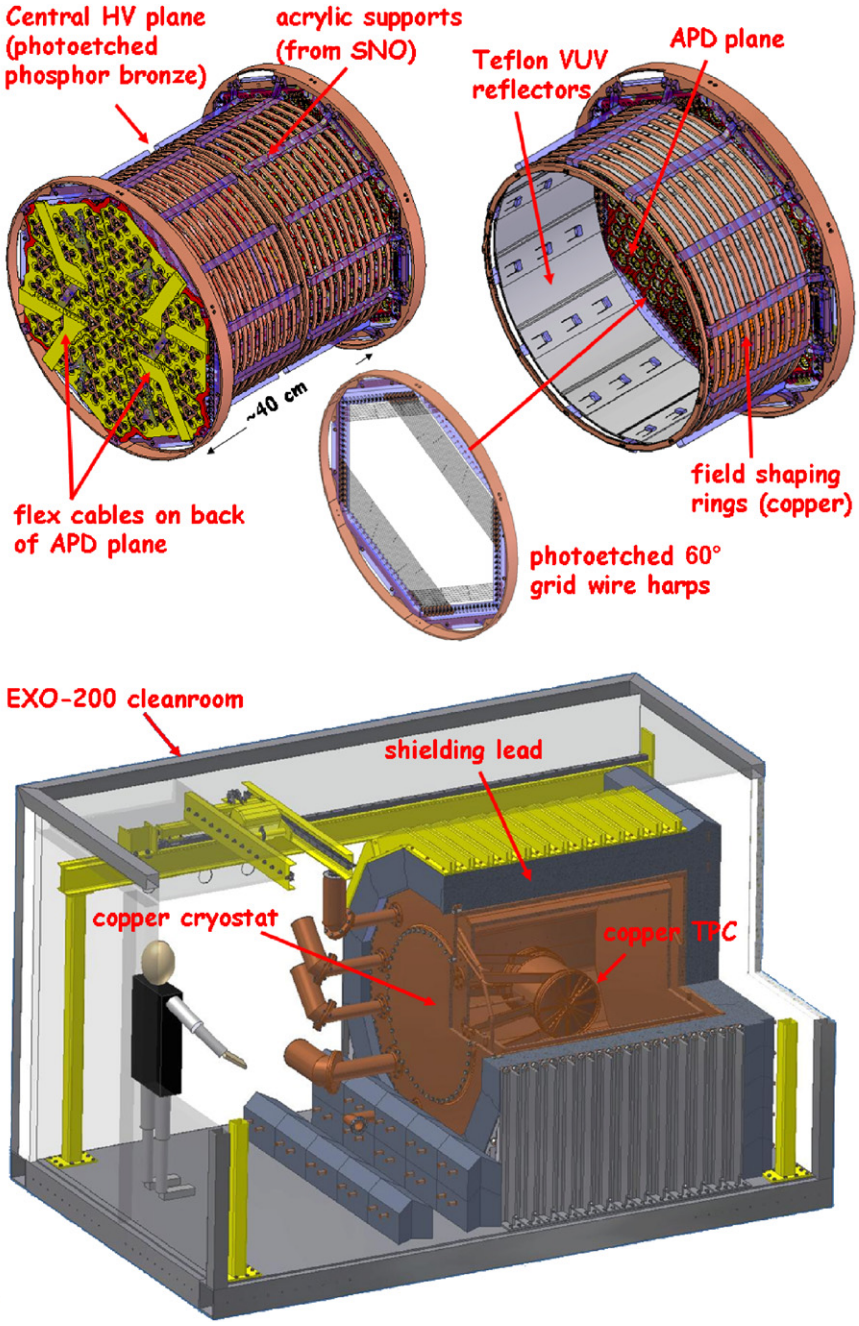

Fig. 1. Top panel: the EXO-200 TPC with major internal parts shown. Bottom panel: cut-away view of the TPC housed in the shielded cryostat. The cleanroom is underground in the Waste Isolation Pilot Plant (WIPP) near Carlsbad, NM with an overburden of 1585^{+11}_{-6} m.w.e. [4].

radioactive impurities, especially the naturally occurring elements K, Th, and U. We performed an extensive campaign of radiopurity measurements to search for and certify a library of suitable materials for every component of the EXO-200 detector. Special attention was given to materials considered for massive parts of the detector and for materials near the active volume or in contact with the xenon.

Our techniques for measuring intrinsic purities include mass spectrometry (MS), neutron activation analysis (NAA), and direct gamma counting. In addition, alpha counting was used to determine ^{210}Pb concentrations in lead. Measurement techniques used for specific samples were selected based on a number of factors and constraints. Both NAA and MS can be used with small sample masses, on the order of a gram. In comparison to NAA, MS is less expensive and faster. Glow-discharge mass-spectrometry (GD-MS) gives results for many elements simultaneously but has relatively poor sensitivities and can only be used with conductive or semi-conductive solids. In contrast, inductively-coupled plasma mass spectrometry (ICP-MS) can have much higher sensitivities, but the difference is large only if preconcentration procedures are used. Only materials which are chemically compatible with these procedures are candidates for ICP-MS. For our U and Th ICP-MS analyses, this implies that samples must be soluble in HNO_3 or possibly in some other acids. NAA can be performed on small samples of many types of materials and can, in some cases, produce the best sensitivities of all known techniques, but the process is relatively costly and slow. Depending on the composition of the material, activation signals from the primary constituents or from uninteresting trace contaminants can interfere with the signals of interest, often resulting in higher than ideal or even useless sensitivity levels. Finally, direct gamma counting can be used to simultaneously measure levels of K, Th, and U (as well other radioactive isotopes) in virtually any material, but requires large sample masses and long measurement times.

MS and NAA assay directly the ^{232}Th and ^{238}U concentrations. However, these isotopes decay initially through low-energy decays below the EXO-200 threshold and through alpha emissions which, as well as having very short ranges, can be rejected by comparison of ionization and scintillation signals. It is subsequent decays of particular daughter isotopes which produce high energy gamma emissions that can penetrate into the detector's interior and contribute to the EXO-200 backgrounds. If all isotopes in a decay chain remain within the same volume, then secular equilibrium is achieved. The activity, and thus concentration, of any isotope can then be inferred from a measurement of the activity or concentration of any other isotope within the same decay chain. However, chemical processes or outgassing can remove radioactive daughter isotopes from materials, thus breaking secular equilibrium. Gamma counting has the advantage that it measures the gamma intensities of the decay products relevant to the EXO-200 backgrounds. For consistency though, data from all techniques used are reported here as total concentrations of the element corresponding to the progenitor isotope. Gamma counting results have thus been converted assuming secular equilibrium in the decay chain. For each of K, Th, and U, natural terrestrial abundance ratios were used to covert from isotopic to total elemental abundances.

Differences in the measurement techniques were weighed against our resources and our requirements for each material. Results are listed in Tables 2 and 3. The tables also include some data (clearly identified) produced by commercial laboratories using similar techniques.

The liquid-xenon TPC of the EXO-200 detector is contained in a thin-walled copper pressure vessel. However, in various phases of the design, we have considered other materials for construction of the vessel. These included quartz, high-purity copper, fluoropolymers, and other plastics. Using NAA, described in Section 5, we found some fluoropolymers, (especially DuPont Teflon TE-6472) in their raw forms, to be among the cleanest solids that we are aware of, both from a radio-purity perspective and also from a general chemical-purity perspective. After careful review and oversight of the sintering process, we also found that finished parts could be produced cleanly. Table 3 entries 41–56 list results for various fluoropolymers in raw form as well as finished products, in some cases both before and after reviewing the sintering process. Detailed descriptions of functional studies of fluoropolymer test vessels are described in Ref. [2].

The TPC contains wire grids for charge collection, and avalanche photo diodes (APDs) for detection of scintillation light. Copper-clad flexible circuits, used in the manufacturing of various signal cables, were analyzed in two steps. First the copper was dissolved in HNO_3 and measured using ICP-MS. The remaining polyimide substrate was then measured using NAA. Germanium counting was also used to analyze whole, unaltered samples of these circuits. Commercial photo-etching processes were investigated for production of the grid wires and APD contacts. Again, by careful oversight, including testing and selection of chemicals (see Table 3 entries 90–96) used in the etching process, we were able to improve the cleanliness of the products. Materials used in the construction of the APDs, including the silicon substrate and the evaporated metal coatings, were individually studied to improve on the cleanliness of the product. Results for APDs produced by Advanced Photonix Inc. (API), using their default material suppliers, are shown in Table 3 entries 131–134. Entries 121–123 show results for aluminum used in the APDs (used in both the Au contacted and Al contacted APDs) and supplied by API's default supplier. Entries 115–120 list measurement results for aluminum replacement candidates procured by EXO.

The EXO-200 TPC is surrounded by a cryogenic heat transfer fluid (HTF) which serves as a thermal bath and

also as a hermetic clean radiation shield. The HTF is contained and cooled in a large copper cryostat surrounded by lead shielding and placed underground in the Waste Isolation Pilot Plant (WIPP) near Carlsbad, NM. Because of the large mass of the HTF (approximately 4.2 tonnes), we made extra efforts to select and certify candidate materials for this use. Measurements of the final candidate material, 3M HFE-7000, are described in more detail in Section 6. Finally the copper cryostat containing the HTF is surrounded by a thick layer of lead shielding. Measurement and selection of lead at every stage of the production process is described in Section 7.

Many other raw materials and parts were studied including vacuum grease, paint, nuts, bolts, and o-rings. All measurements were selected and prioritized as needed for the specific construction and scheduling needs of EXO. In some cases, materials with unknown origins were tested for use in EXO-200. We report these results here because they give useful impressions of the general trends and achievable purity levels in various types of materials.

2. Handling and surface cleanliness

Surface cleanliness of all samples is a concern for all analysis methods used. Although we normalize most results to the sample masses, assuming that the concentrations are intrinsic to and homogenous throughout the materials, it is clear that positive readings can also come from surface contaminants.

For measurements of raw materials, extensive surface cleaning was performed and samples were handled in cleanroom environments. Typical cleaning procedures included extended soaking in solvents with sonic agitation, as well as extended soaking in 0.1–3 M (or higher for NAA preparation of some materials) nitric acid solutions with certified purity levels. Within a few variations, depending on the material properties, cleaning procedures were followed consistently to assure reproducibility. The effectiveness of the cleaning procedures is demonstrated by the stringent contamination limits set by the most sensitive measurements of the cleanest materials.

When analyzing finished parts (nuts, bolts, o-rings, etc.), care was taken to match the cleaning procedures of the analysis techniques to those that were or will be used for the actual installed parts. In most cases these procedures were similar to those used for analysis of raw materials. In some cases however, due to time, volume, or integrity constraints, it was not possible to perform the full cleaning procedure. Especially for non-critical parts with relatively high tolerable activities, if the parts could be well certified using less stringent cleaning procedures, then some burden or concern could be removed from the construction process.

Specifically, most EXO-200 finished parts were surface cleaned using the following treatment with high purity solvents targeting organic, metallic, and ionic surface impurities:

(1) Acetone rinse followed by ethanol (or methanol) rinse to remove any grease left over from machining or touching. Small parts underwent ultrasonic cleaning for about 15 min while immersed in each solvent, often followed each time by a rinse in the same solvent.
(2) 0.1–1 M HNO_3 rinse to dissolve metallic contamination. For metallic parts light etching results in removal of the surface. Small parts were fully immersed in acid.
(3) Deionized water rinse following the etch. Small parts were dried in a vacuum oven; large parts were left to dry in a cleanroom.

For thin photo-etched phosphor–bronze TPC parts, we found high levels of U which appeared to be surface contamination resulting from the commercial etching procedure. We were able to reduce the U levels by requesting the use of fresh chemicals in the etching process (compare entries 93 and 94 of Table 3) in combination with use of an expanded cleaning procedure which we developed to maximize cleaning effectiveness while minimizing loss of material. These parts were first rinsed in methanol followed by deionized water and then rinsed three times in 3M HNO_3 for 10 min, followed each time by a further rinse in deionized water. This procedure was used to obtain the result in Table 3 entry 89; a 15% loss of sample mass was observed.

After surface cleaning, parts were double bagged (when practical according to size) and were only touched with disposable powder free gloves to prevent re-contamination.

Surface cleanliness of large parts was directly verified by means of wipe testing with Whatman 42 paper filters. The Th and U content of the filters was determined, after ashing, by means of ICP-MS. To reduce the blank concentrations, the filters were soaked for 24 h in 1 M HNO_3 followed by thorough rinsing with deionized water and drying. Analysis of blank filters yielded Th and U masses of 0.27 ± 0.06 and 3.0 ± 0.6 ng per filter, respectively, before acid cleaning and yielded 0.31 ± 0.02 and 0.15 ± 0.03 ng after acid cleaning. To facilitate transfer of surface activity onto the filter paper, the surface to be tested was wetted with either alcohol or 0.1 M nitric acid. The fluid was spread over some surface area and then absorbed with the filter paper. Blank filters were always analyzed to control the filter paper background.

After drying, the filter paper samples were accurately weighed, transferred into porcelain crucibles, and placed in a muffle furnace at 200 °C for 20 min. The temperature of the furnace was then gradually raised at a rate of approximately 10 °C/min with pauses for 30 min at 300 and 400 °C and finally raising the temperature to 500 °C where it was maintained for about 1 h. The crucibles were then removed from the furnace and allowed to cool down. After the samples were cooled, 10 ml of 3M nitric acid was added to each crucible, evaporated to near dryness on a hotplate, and reconstituted to 10 ml with 0.5% nitric acid.

Table 1
Th and U surface contamination as determined by wipe testing

Sample	Th (pg/cm^2)	U (pg/cm^2)
Xenon piping, burst disk, after cleaning[a]	5.8±0.2	1.2±0.1
Bottom inner surface of outer cryostat, before cleaning[a]	380±5	140±3
Top inner surface of outer cryostat, before cleaning[b]	2.6±0.2	0.46±0.04
Top outer surface of outer cryostat, after cleaning[b]	0.60±0.09	0.21±0.05
Jehier super insulation from top of cryostat, after alcohol rinse[b]	5.9±0.2	1.6±0.1
Wessington Cryogenics HFE storage dewar, manufacturer cleaning with wipes soaks and pressure washing[a]	215±12	43±6

Blanks have been subtracted.
[a]The filter was wetted with ethanol before wiping.
[b]The filter was wetted with 0.1 M HNO_3 before wiping.

The Th and U content of the filters was determined by means of ICP-MS. Recovery tests were performed where the filter papers were spiked with known concentrations of the analytes. Complete recovery (>94%) was obtained.

Table 1 summarizes the results for various wipe tests performed on EXO-200 samples.

3. Mass spectrometry

ICP-MS offers sub pg/ml detection limits for U and Th with minimal analysis time. However, one of the main limitations of this technique is the need for sample preparation prior to analysis, as higher levels of matrix components can give rise to deposition of matrix constituents on the sampler and skimmer cones of the spectrometer. Thus, a dissolved sample may need to be diluted in order to lower its total dissolved solids content to <1%, clearly degrading achievable detection limits. One way of overcoming this drawback is to undertake prior separation of the analytes from the matrix. Several methods have been used for this purpose including coprecipitation [5–7], liquid–liquid extraction [8–10], distillation [11], and ion-exchange [12,13] which was used in this work (see Section 3.1). These techniques often require longer analysis times and give rise to additional analytical problems, including contamination during sample pretreatment and increased blank levels, which must be carefully controlled.

Direct analysis of solid samples can be advantageously performed, without chemical sample preparation, by GD-MS [14,15] wherein the sample functions as the cathode of the discharge, making this approach particularly suitable for the analysis of high-purity metals.

3.1. ICP-MS

An ELAN DRC II (dynamic reaction cell) ICP-MS (Perkin-Elmer Sciex) equipped with a cyclonic glass spray chamber and a pneumatic nebulizer (Meinhard) was used for the determination of U and Th with sensitivities as low as 10^{-12} g/g. The ICP-MS operating parameters were selected to maximize sensitivity for U and Th. Samples were acid digested and then the analytes separated using a chromatography resin (UTEVA from Eichron). The U fraction was eluted from the resin with 15 ml of 0.02 M HCl, and the Th fraction was subsequently eluted with 30 ml of 0.5 M oxalic acid. Both fractions were evaporated to near dryness; the thorium fraction was decomposed with 24 ml of a mixture of concentrated HNO_3/30% and H_2O_2 (1:1). Both fractions were reconstituted to 2 ml with 0.5% nitric acid. U and Th were measured at masses 238 and 232, respectively. The procedure is described in more detail in Ref. [16].

For the determination of K concentrations at levels below 10^{-6} g/g, samples were acid digested, diluted 100-fold and subsequently analyzed by DRC-ICP-MS using an ultrasonic nebulizer as a sample introduction system. ^{39}K suffers from interferences from ^{38}Ar ^{1}H^{+} and ^{40}Ar. These interferences were overcome with the use of chemical resolution, a process used to selectively remove interfering polyatomic or isobaric species from the ICP-MS ion beam using controlled ion–molecule chemistry. Ammonia (at 0.5 ml/min flow rate) was used as a reaction gas as it reacts with the Ar-based interferences to form new species that do not interfere with ^{39}K. Samples were introduced to the ICP-MS with an ultrasonic nebulizer in order to further decrease the hydride formation and consequently the interference to ^{39}K. The samples were nebulized by a piezoelectric crystal transducer. The nebulized aerosol was passed through a heated chamber and condenser where the solvent vapor was removed.

Uncertainties in the ICP-MS results were dominated by variability in the subtracted backgrounds, as observed by analysis of clean digestion acids, and to a lesser extent by scaling errors due to calibration uncertainties. All known uncertainties are included in the tabulated results.

3.2. GD-MS

A VG 9000 GD-MS (Thermo Electron Corp., UK) was used for direct analysis of solid samples (conducting and semiconducting solids). The instrument is capable of detecting impurities directly in the solid from the percent level down to below 10^{-9} g/g in a single run, allowing for a rapid turn around of submitted samples. It relies on a DC glow discharge ion source coupled to a high resolution magnetic sector analyzer in reverse Nier Johnson geometry with electron multiplier detection at nominal resolution $R = 3000$, where $R \equiv m/\delta m$, and δm is the resolvable mass difference at an ion mass of m. Atoms were sputtered in a low-pressure DC argon discharge, subsequently ionized in this plasma, and extracted into the MS for separation and detection. Test portions of the samples were prepared by cutting pins of approximately $2.5 \times 2.5 \times 20$ mm and subjecting them to a careful surface leach in dilute

ultrapure nitric acid. Following a rinse with ultrapure water, the samples were permitted to air dry in a laminar-flow class-100 clean-bench, where they were subsequently mounted into the DC ion source. Once under vacuum, and then Ar purged, the glow discharge was ignited. Any surface contamination on the test samples was removed by a 30 min pre-burn in the plasma before data acquisition was initiated. Typically 300 mass spectral scans were acquired, each having a 50 ms dwell or integration time. The GD-MS instrument was calibrated with the use of a variety of reference materials used to establish relative sensitivity factors to provide semiquantitative analysis, results of which are deemed to be (conservatively) within a factor of 2 of the real value of the concentration of the analyte. GD-MS is free from the matrix dependence response plaguing most other elemental analysis techniques, minimizing the need for matrix matched standards.

4. Gamma counting

For EXO, gamma counting was used primarily for small non-critical components, such as screws, washers, etc., which contribute little to the EXO-200 detector mass. This technique was also used for cross checking other measurements of bulk materials, in particular measurements of the copper for the TPC vessel and cryostat, and of the shielding lead.

A few non-critical materials were counted in above ground detectors but most were counted underground in the Vue-des-Alpes underground laboratory. The overburden is 230 m of rock (600 m.w.e.), so that the nucleonic component of the cosmic rays is completely eliminated. The muon flux is attenuated by a factor of 1000. The detector itself is a p-type coaxial germanium detector with a useful volume of 400 ml. The geometry is indicated in Fig. 2. The germanium crystal is housed in a cryostat made from highly purified Pechiney aluminum. All materials entering in the construction of the detector were themselves selected for low activity. The energy resolution is 2.2 keV at 2 MeV. The detector is protected against local activities by a shielding composed of 15 cm of OFHC copper and 20 cm of lead. The shielding is contained in an air-tight aluminum box which is slightly overpressurized with boil-off nitrogen from the detector's liquid-nitrogen dewar, thus preventing radioactive radon gas from entering the detector volume. As shown in Fig. 2, a small volume is free around the sensitive part of the detector in order to position samples to have the best possible solid angle. Small samples were placed on top of the cryostat whereas larger ones were arranged on top and around the cylindrical part of the cryostat. This arrangement has the extra advantage that it reduces self absorption of gammas in the sample.

Prior to insertion, samples were ultrasonically cleaned in an alcohol bath. Data taking was started one day after closing the shielding to ensure that all radon gas was flushed out. Normally data were accumulated for a period of one week for each sample. Detector backgrounds limit the effectiveness of longer accumulation times. In critical cases, (measurements of lead and copper) data were accumulated for periods as long as a month. The contribution of a sample is obtained by subtracting the background spectrum taken without any sample (Fig. 3). The background was measured at regular intervals although it was found to be very stable.

For each sample, the geometry was entered in a simplified way into a GEANT3 based Monte Carlo simulation which contained also the detector configuration. The acceptance as a function of energy of the full energy gamma peaks was computed and used to translate the observed intensity of a transition, or the upper limit on it, into a specific activity. The computed acceptance was cross checked by exposing the detector to calibrated gamma sources. The sensitivity depends on the sample mass and configuration, which affect the solid angle and the self absorption. For transitions with several gamma emissions contributing in parallel, or by cascade, the peak intensities were combined. The best sensitivity was

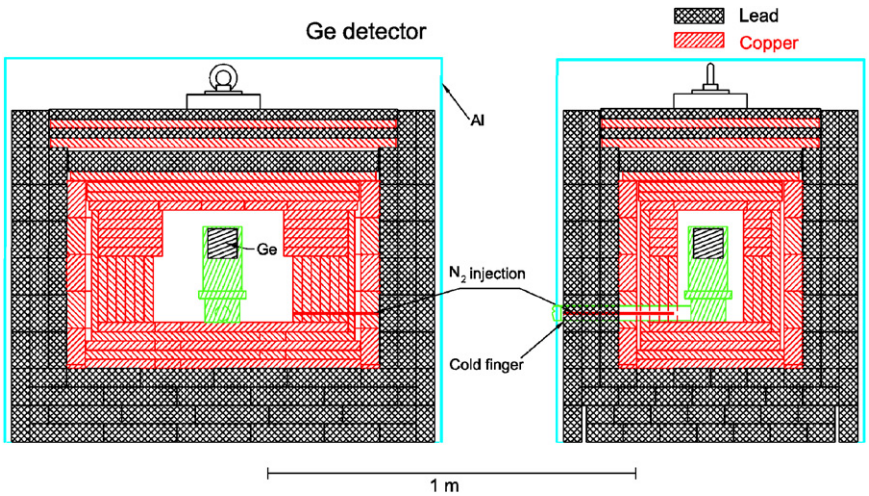

Fig. 2. The germanium detector in its copper and lead shielding. The aluminum radon containment box is also shown.

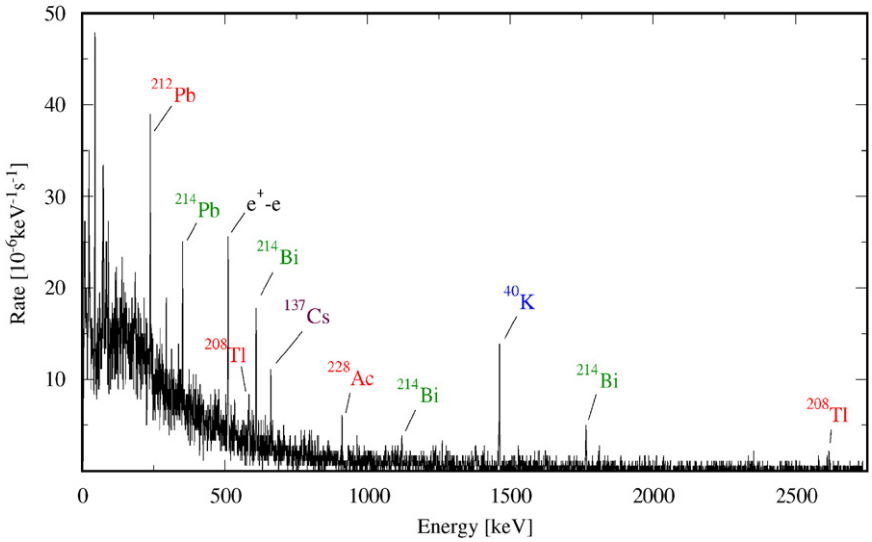

Fig. 3. Underground germanium background spectrum, measured with no sample for 672 h. Gamma lines from natural activities, namely the ^{232}Th (^{208}Tl, ^{228}Ac, ^{212}Pb) and ^{238}U (^{214}Bi, ^{214}Pb) chains, ^{40}K, as well as the ^{137}Cs line from an artificial activity, are indicated.

achieved with copper samples with masses of several kilograms (see Table 3 entry 2). The quoted errors include statistical uncertainties as well a systematic error, dominated by the acceptance, which is estimated to be of order 10%.

5. Neutron activation analysis

We have used the MIT Reactor (MITR) Lab to neutron activate many material samples. After activation and shipping, gamma emissions from the unstable activation products were observed at an EXO lab using the same germanium detector as that used for the above ground direct gamma counting mentioned in Section 4. By observing gamma energies, intensities, and decay half-lives it is possible to identify and measure the activities of many of the neutron activation products. In practice, good spectral analysis in the presence of a multitude of gamma lines is not trivial and can have a significant impact on sensitivity and accuracy.

In order to maximize use of data (and thus sensitivity), as well as to simplify the analysis, a spectral fit was constructed using the most global set of experimental parameters as was practical. Multiple energy regions of interest were defined, each having three background parameters. Two parameters for a linear energy-calibration and two global energy-dependent peak-width parameters were used in the fit as well as one activity parameter for each isotope. Care was taken to convert energy regions of interest to channel regions in a way which would not change the data set while minimizing the fit, which included the calibration parameters. Peaks were defined with fixed energies, and each rate was associated with an isotopic activity via the product of the branching ratios and the detector efficiency at the relevant energy. By parameterizing activities instead of peak areas, all peaks associated with a single isotope could be used to simultaneously constrain an activity. The inclusion of strong, known peaks in the fits resulted in automatic energy and resolution calibration. Interleaved calibration data could also be used to introduce constraint terms for particularly in-active samples after long delay times. By allowing the energy calibration to float in a constrained manner while keeping peak energies fixed, subtleties of explicitly constraining peak centroids were avoided, and strong correlations in peak-position uncertainties were retained. The fit procedure was automated to produce results for data files taken in temporal sequence. This produced time-dependent decay curves for each activity which could be fit to determine initial activities and half lives. A calibration gamma spectrum taken from the interactive software interface is shown in Fig. 4. The time series of different activities shown in Fig. 5 were found by combining the data from this and other spectra collected in sequence.

Elemental concentrations were inferred using tabulated neutron capture cross-sections folded with a standard reactor neutron spectrum. We assume that the relative isotopic abundances within the samples are given by the natural terrestrial abundance ratios. The reactor neutron flux was periodically calibrated by activating samples of NIST coal fly-ash Standard Reference Material 1633b, which has certified known concentrations of several NAA-detectable elements including K, Th, and U. Repeated calibrations showed a linear correlation between reactor power and thermal neutron flux. For activation runs without a fly-ash calibration sample, this correlation was used together with the stated reactor power at the time of activation. The fractional flux of epi-thermal neutrons was found to have only little dependence on the reactor power. Due to the large resonance integral in the neutron capture cross-section of ^{238}U, this nuclide is quite sensitive to this detail. Results listed in Table 3 include a statistical

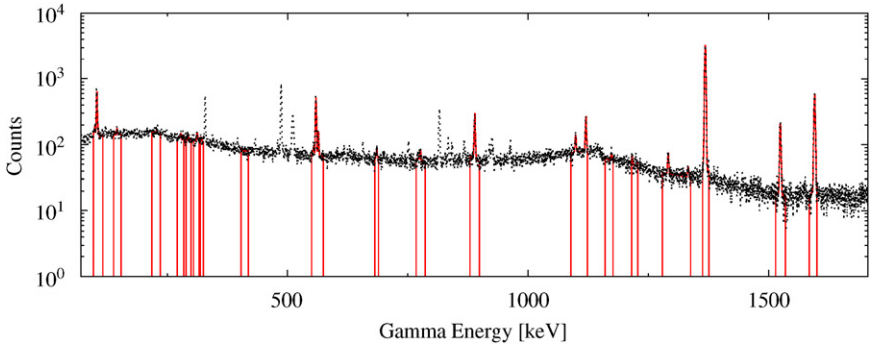

Fig. 4. Partial neutron-activated fly-ash gamma spectrum (dotted line) with global fit (solid line). The parameterization for this fit described backgrounds for 23 regions of interest and 62 peaks with rates linked to 31 activity parameters.

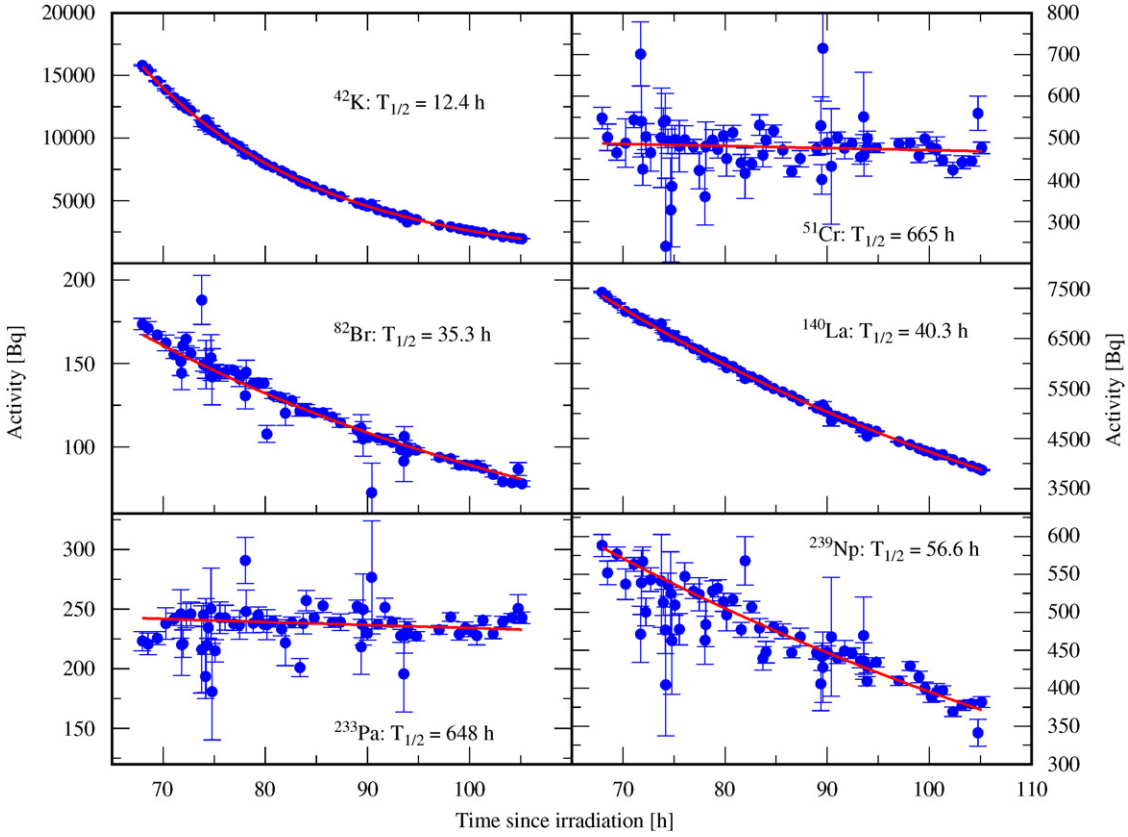

Fig. 5. Time development of activities in a neutron-activated fly-ash calibration sample as determined from a sequence of spectral fits (See Fig. 4). The points are the data; the curves are fit to exponential decays with the half-lives fixed to the values shown.

uncertainty and a systematic uncertainty, which in most cases is dominated by a 10% error associated with flux variations and with solid angle variations during germanium counting.

After demonstrating good reproducibility over the course of several years, calibrations were recently performed only about once per year. However, the latest calibration, performed in September of 2006 showed that the ratio of total flux to epi-thermal flux was about a factor of 3 lower than found in the previous calibration, performed in March of 2005. Data taken in the interval between these two calibrations are thus subject to significantly higher systematic uncertainties. The affected measurements are indicated in Table 3. The quoted results use the original 2005 calibration and do not include this added flux uncertainty. Using the 2006 calibration, results are found to be higher by factors of approximately 1.1, 1.3, and 2.2 for K, Th and, U, respectively.

NAA results using the same facility and essentially the same techniques have been reported in the past [17] in more detail. In Ref. [17], NAA measurement limits on the order of 10^{-14}–10^{-15} g/g of Th and U were achieved for KamLAND liquid scintillator, demonstrating the potential power of the technique. However, achieving these

sensitivities required a specialized measurement campaign customized to the material of interest. Specifically the preconcentration and chemical separation techniques used in Ref. [17] were not employed, with one exception described below, for measurements in the present work. When surveying a large number of samples, such specialized techniques are not practical. Many systematic details of the technique including sample mass, containment vessel choice, and irradiation time, were varied to account for properties of individual materials and our specific analysis needs and goals.

6. Heat transfer fluid

3M Novec HFE-7000, 1-methoxyheptafluoropropane, serves as a HTF and as passive shielding in EXO-200. Because of its large mass and close proximity to the active detector volume, the allowable tolerances for U and Th contamination in this material are particularly stringent. An extended effort was made to improve analysis sensitivities for this material. Initially a standard NAA was performed producing limits for K, Th, and U concentrations which were among the lowest of any of the materials measured (see Table 3 entries 135–138). We also found that HFE-7000 has very low levels of other foreign elements, making it one of the most pure materials that we have studied.

In order to make further improvements we preconcentrated the HFE-7000 by evaporation, reducing its mass by a factor of 1000. We attempted to quantify the Th and U retention of the evaporation process by mixing organometallic standards [17] with the HFE-7000. These studies were unsuccessful, but indicated a very low solubility of actinides in HFE-7000. For indirect verification of metal retention, ^{220}Rn gas was bubbled through an HFE-7000 mixture. This loaded the HFE-7000 with ^{212}Pb which was detectable in a gamma detector before and after evaporation. The concentrate was transferred from the evaporation vessels to a separate test tube and further evaporated to produce a dry residue. Approximately 20% of the ^{212}Pb was retained in the concentrate residue. With large systematic uncertainties, the amount of ^{212}Pb on the surfaces of the evaporation vessels was found to be consistent with the remaining 80% of ^{212}Pb initially introduced. With the assumption that this 20% evaporation retention also applies for Th and U, we derived strict limits for their concentrations in HFE-7000 as shown in Table 3 entry 139.

7. Shielding lead

To find a suitable shielding lead we needed to select, as usual, for low concentrations of K, Th, and U, but also for low levels of ^{210}Pb. ^{210}Pb and its shorter lived decay product ^{210}Po are primarily beta and alpha emitters, respectively. However, because of their potentially high activities, long ranged Bremsstrahlung radiation as well as a very weak gamma line at 803 keV can potentially penetrate shielding at rates high enough to impact EXO-200 backgrounds in the energy range of the ^{136}Xe two-neutrino decay mode.

To address this additional concern we used a 1700 mm^2 ion-implanted silicon detector to observe the 5304 keV alpha particles from the decay of ^{210}Po in several different supplies of lead. The detector efficiency was calibrated with Doe Run lead batches previously analyzed by Physikalisch-Technische Bundesanstalt (PTB) in Germany. Background measurements were taken by replacing the lead samples with a silicon wafer.

The EXO-200 shielding lead was selected, acquired, smelted, cleaned, and machined at JL Goslar in Germany. Many batches of Doe Run lead were smelted together into three homogenized batches. We analyzed the ^{210}Po activities of samples from all candidate batches (about 20) of Doe Run lead purchased and from samples of all three homogenized batches. We found that the ^{210}Po activities of most candidate batches varied only within the

Table 2
^{210}Po (from ^{210}Pb decay) activities in various lead sources as measured by alpha counting

Lead source	Activity (Bq/kg)
JL Goslar, Doe Run, EXO smelting lot 3-708	20±5
JL Goslar, Doe Run, EXO smelting lot 3-707	17±5
JL Goslar, Doe Run, EXO smelting lot 3-706	17±4
JL Goslar, un-smelted Doe Run lot 9273	25±4
Tako Esco Ltd	165±33
JL Goslar, Boliden	18±3
Plombum, VG1	5.9±0.9
Plombum lead from Integrated Ocean Drilling Program	5.4±1.3
JSC Industrial Corporation, lead quality C1	1265±183

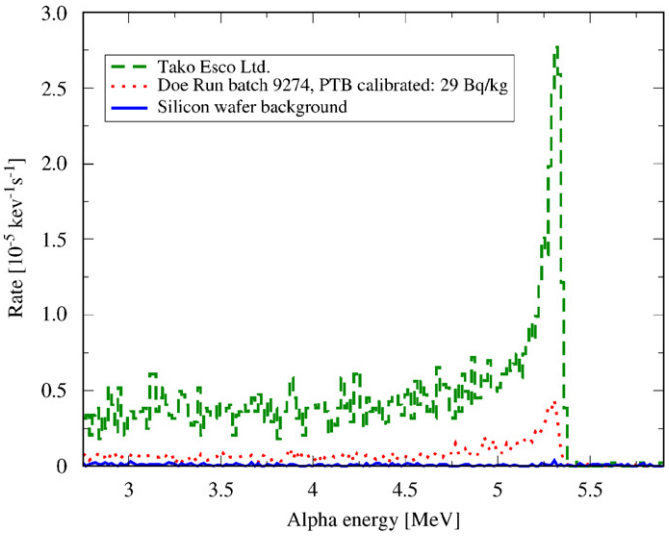

Fig. 6. Spectra from alpha counter including Doe Run batch 9274, which was a calibration batch measured by PTB (28.9 ± 2.9 Bq/kg), as well the spectrum from lead supplied by Tako Esco Ltd., and a background spectrum. The spectra are binned in groups of ten channels.

Table 3
Measurement results for K, Th, and U concentrations in a variety of materials

#	Material	Method	K conc. (10^{-9} g/g)	Th conc. (10^{-12} g/g)	U conc. (10^{-12} g/g)
	Bulk copper				
1	Norddeutsche Affinerie, NOSV copper made May 2002	Shiva Inc. GD-MS	0.4	<5	<5
2	Norddeutsche Affinerie, NOSV copper made May 2002	Ge	<120	<35	<63
3	Norddeutsche Affinerie OFRP copper made May 2006, batch E263/2E1	ICP-MS	<55	<2.4	<2.9
4	Norddeutsche Affinerie OFRP copper made May 2006 batch E262/3E1	ICP-MS	<50	<2.4	<2.9
5	Rolled Norddeutsche Affinerie OFRP copper, May 2006 production. Rolled by Carl-Schreiber GmbH	ICP-MS	–	<3.1	<3.8
6	TIG welded Norddeutsche Affinerie OFRP copper made May 2002. No cleaning after welding. Results are normalized to length of weld	ICP-MS	–	<9.8 pg/cm	10.2 ± 3.4 pg/cm
7	Valcool VNT 700 metal working lubricant, concentrate	A.G. Ge	$38\,000 \pm 11\,000$	$<10\,000$	<3700
8	Water alcohol mixture, lubricant for machining of Cu parts	A.G. Ge	$<44\,000$	$<18\,000$	<3800
	Lead				
9	JL Goslar cutting oil. Used for cutting 98% distilled water, 2% cutting oil. ^{60}Co: <1.8 mBq/kg, ^{137}Cs: <12 mBq/kg	Ge	$93\,500 \pm 1000$	<790	3650 ± 510
10	Paint for lead bricks, JL Goslar, type: Glasurit MS-Klarlack. Proportions: 2 paint, 1 hardener, 0.1 solvent	Ge	720 ± 170	<170	790 ± 90
11	EXO Pb, JL Goslar smelting lot 3-706	ICP-MS	–	<1	<1
12	EXO Pb, JL Goslar smelting lot 3-706	GD-MS	<15	<6	<6
13	EXO Pb, JL Goslar smelting lot 3-707	ICP-MS	–	<1	<1
14	EXO Pb, JL Goslar smelting lot 3-707	GD-MS	<10	<5	<6
15	EXO Pb, JL Goslar smelting lot 3-708	ICP-MS	–	<1	<1
16	EXO Pb, JL Goslar smelting lot 3-708	GD-MS	<7	<7	<8
17	JL Goslar production, Doe Run, Lot 9273	ICP-MS	–	<3	<3
18	JL Goslar production, Doe Run, Lot 9273	GD-MS	<5	<10	<10
19	Vulcan Lead, source Doe Run. Lot ID D9258	GD-MS	5	<5	<5
20	Vulcan Lead, source Doe Run. Lot ID D9146	GD-MS	5	<4	<5
21	Vulcan Lead, source Doe Run. Lot ID D9119	GD-MS	<1	<4	<4
22	Vulcan Lead, source Doe Run. Lot ID D9086	GD-MS	<0.5	<5	<6
23	Plombum, VG2 lead	Shiva Inc. GD-MS	2.1	270	<100
24	Plombum, VG2 lead	ICP-MS	–	<2	<0.5
25	Plombum, VG2 lead	GD-MS	<1	<9	<20
26	Plombum, VG2 lead	Ge	<3.0	<11	<21
27	Plombum, VG1 lead	GD-MS	<2	<7	<10
28	Teck-Cominco low alpha lead	GD-MS	<2	<4	<4
29	Boliden lead	GD-MS	<4	<7	<7

Table 3 (*continued*)

#	Material	Method	K conc. (10^{-9} g/g)	Th conc. (10^{-12} g/g)	U conc. (10^{-12} g/g)
30	Princess Louisa Pb (1743)	GD-MS	<0.9	<8	<10
31	Princess Louisa Pb (1743). Data from D. Arnold [18]	PTB Ge [18]	<3600	<3200	3600 ± 740
32	JSC Industrial Corporation, lead quality C1	Shiva Inc. GD-MS	0.52	110	<10
33	JSC Industrial Corporation, lead quality C1	Ge	<520	790 ± 150	8500 ± 900
34	MUNU lead pellets. ^{60}Co: 1.4 ± 0.3 mBq/kg	Ge	710 ± 120	<320	970 ± 140
35	Cominco low alpha Pb	NAA	–	<22	–
36	Boliden Pb	NAA	–	<22	–
	Plastics				
37	SNO acrylic, batch 48, panel 09	NAA[a]	<2.3	<14	<24
38	SNO acrylic. Data from J. Boger et al. [19]	SNO NAA [19]	–	<1.1	<1.1
39	DuPont Vespel, plaque 1	NAA[a]	46 ± 5	<21	<29
40	DuPont Vespel. plaque 2	NAA[a]	209 ± 22	<10	<19
41	Stanford stockroom virgin Teflon	NAA	16 ± 2	122 ± 12	<20
42	DuPont Teflon TE-6472, raw material	Ge	<740	<112	<200
43	DuPont Teflon TE-6472, raw material	NAA[a]	1.8 ± 0.2	<0.26	<0.78
44	APT supplied DuPont TE-6472 raw material	NAA	2.5 ± 0.8	<1.8	<4.4
45	Saint Gobain supplied DuPont 440-HPB PFA, raw material, lot: 0102THPP07	NAA	<0.9	<1.9	<1.8
46	Saint Gobain supplied DuPont 440-HP PFA, raw material, lot: 0401THP053	NAA	6.7 ± 0.9	–	<5.9
47	Saint Gobain supplied DuPont 450-HPB PFA. Material finished using supplier's default procedures	NAA	740 ± 77	65 ± 6.5	<75
48	Saint Gobain DuPont 440-HP PFA. Material finished using customized procedures	NAA	5.3 ± 1.0	<13.3	<3.0
49	Saint Gobain supplied Daikin Neoflon PFA AP-231SH, lot A31SR 29010 MFR 1.76, raw pellets	NAA[a]	81 ± 8	29.3 ± 3.5	48.1 ± 7.8
50	Saint Gobain supplied Daikin Neoflon PCTFE (Kel-F), M-400H, raw material. ^{60}Co: <0.58 mBq/kg	Ge	<980	<570	450 ± 100
51	Saint Gobain supplied Daikin Polyflon PTFE M-112, raw material	NAA[a]	<12	<4.9	<7.0
52	Saint Gobain supplied Daikin Polyflon PTFE M-111, raw material	NAA[a]	<4.9	<2.6	<7.2
53	Saint Gobain supplied 3M TFM-1700, raw material	NAA	2220 ± 230	–	<970
54	Saint Gobain supplied 3M TFM-1700 Teflon Material finished using supplier's default procedures	NAA	3100 ± 300	<5.4	<10
55	Saint Gobain supplied 3M TFM-1700. Material finished using customized procedures	NAA	2900 ± 300	–	<128
56	APT supplied DuPont, NXT-75 raw Teflon	NAA	3.2 ± 1.3	<1.6	<1.9

57	General Electric Polycarbonate104-111N raw pellets, grade 104-111N	NAA	107 ± 53	<33	<105
58	Dow Corning Polycarbonate PC20010 raw pellets, grade PC20010	NAA	18 ± 2	<33	<6.5
59	Bayer Makrolon finished Polycarbonate plastic	NAA	53 ± 5	204 ± 20	<136
60	Bayer Makrolon raw Polycarbonate pellets	NAA	288 ± 29	<21	<3.7
	Quartz				
61	Corning high purity quartz	NAA[a]	1.05 ± 0.24	1.8 ± 0.5	270 ± 27
62	Dynasil quartz	NAA[a]	1.16 ± 0.28	–	226 ± 22
63	Saint Gobain Spectrosil quartz	NAA	<3	12 ± 2	<4.6
64	Kvartzsteklo, fused silica type KY1	NAA	21 ± 3	23 ± 3	17 ± 4
65	Heraeus 2 quartz	NAA	2.0 ± 0.5	6.7 ± 1.2	5.5 ± 2.2
66	Heraeus 311 quartz	NAA	5.8 ± 0.8	14.1 ± 2.1	4.9 ± 2.0
67	Heraeus Suprasil quartz	NAA	–	59 ± 14	21 ± 9
	Adsorbends				
68	Selecto 32–63 μm Silica gel, acid washed	A.G. Ge	$<54\,000$	$63\,000 \pm 7600$	$46\,000 \pm 3800$
69	Selecto 32–63 μm Silica gel	A.G. Ge	$<122\,000$	$167\,000 \pm 96\,000$	$152\,000 \pm 37\,000$
70	Selecto, Alusil 70 (alumina gel)	A.G. Ge	$(1.5 \pm 0.2) \times 10^8$	$<160\,000$	$374\,000 \pm 58\,000$
71	Selecto, Alusil 40 (alumina gel) no K added	A.G. Ge	$(5.3 \pm 0.1) \times 10^7$	$429\,000 \pm 78\,000$	$140\,000 \pm 44\,000$
72	Cu–Mn Catalyst T-2550, Sued Chemie	A.G. Ge	$(1.1 \pm 0.1) \times 10^6$	$146\,000 \pm 15\,500$	$48\,000 \pm 8600$
73	Carbo-Act International (NL) activated charcoal	NAA	103 ± 11	111 ± 18	206 ± 22
74	Carbo-Act International (NL) activated charcoal	A.G. Ge	$<145\,000$	$<74\,000$	$<65\,000$
75	Kansai MAXSORB activated charcoal	NAA	$496\,000 \pm 25\,000$	$81\,000 \pm 41\,000$	–
76	Kansai MAXSORB activated charcoal	A.G. Ge	$622\,000 \pm 81\,000$	$205\,000 \pm 27\,000$	$44\,000 \pm 11\,000$
	Phosphor–bronze photo-etching				
77	0.005 in. thick phosphor–bronze from Sequoia Metals	ICP-MS	150 ± 60	14 ± 3	87 ± 3
78	0.005 in. thick phosphor–bronze for TPC grid wires from E. Jordan Brooks	ICP-MS	<80	27 ± 2	<1
79	0.005 in. thick phosphor–bronze for TPC grid wires from E. Jordan Brooks. ^{60}Co: <0.3 mBq/kg, ^{137}Cs: <1.9 mBq/kg	Ge	<460	<135	<123
80	0.01 in. thick phosphor–bronze for APD spiders from E. Jordan Brooks	ICP-MS	<80	2.5 ± 0.9	2.6 ± 1
81	Uncleaned photo-etched phosphor–bronze TPC grid wires from Newcut Inc. Base material is entry 79	ICP-MS	<80	250 ± 15	6600 ± 40
82	Uncleaned photo-etched phosphor–bronze TPC grid wires from Vaga Industries. Base material is entry 79	ICP-MS	200 ± 50	56 ± 1	358 ± 5
83	Cleaned photo-etched phosphor–bronze TPC grid wires from Vaga Industries. Base material is entry 79	ICP-MS	<90	47 ± 2	320 ± 2
84	Uncleaned photo-etched phosphor–bronze APD spider contacts from Newcut Inc. Base material is entry 80	ICP-MS	<60	77 ± 8	3300 ± 20

Table 3 (*continued*)

#	Material	Method	K conc. (10^{-9} g/g)	Th conc. (10^{-12} g/g)	U conc. (10^{-12} g/g)
85	Cleaned photo-etched phosphor–bronze APD spiders from Newcut Inc. Base material is entry 80	ICP-MS	<60	65 ± 5	1700 ± 10
86	Uncleaned photo-etched phosphor–bronze APD spiders from Vaga Industries. Base material is entry 80	ICP-MS	<60	9 ± 1	113 ± 1
87	Cleaned photo-etched phosphor–bronze APD spider contacts from Vaga Industries. Base material is entry 80	ICP-MS	<70	8 ± 1	71 ± 3
88	Uncleaned photo-etched phosphor–bronze APD spider contacts from Vaga Industries using selected chemicals. Base material is entry 80	ICP-MS	–	23 ± 3	317 ± 25
89	Cleaned photo-etched phosphor–bronze APD spider contacts from Vaga Industries using selected chemicals. Base material is entry 80	ICP-MS	–	10.6 ± 2.0	12.4 ± 2.1
90	RD Chemical Company RD38, Vaga Industries photo-etch chemical	A.G. Ge	$<124\,000$	$<74\,000$	–
91	DI water for Vaga Industries photo-etch	A.G. Ge	$<57\,000$	$<27\,000$	<9200
92	Solid soda ash from Hill Brothers Inc., Vaga Industries photo-etch chemical	A.G. Ge	$<13\,200$	$<52\,000$	$39\,300 \pm 11\,300$
93	Used ferric chloride from Phibro Tech Inc., Vaga Industries photo-etch chemical	A.G. Ge	$26\,100 \pm 7300$	$63\,200 \pm 7900$	$20\,300 \pm 2700$
94	Fresh ferric chloride from Phibro Tech Inc., Vaga Industries photo-etch chemical	A.G. Ge	$<29\,000$	$<12\,300$	<3300
95	RD Chemical Company RD87, Vaga Industries photo-etch chemical	A.G. Ge	$<54\,000$	$<89\,000$	–
96	Alcohol, Vaga Industries photo-etch chemical	A.G. Ge	$<49\,000$	$<34\,000$	$<10\,100$
97	California Fine Wire, 20 mil phosphor–bronze wire, annealed. Lot #24987	GD-MS	<23	<20	<20
98	California Fine Wire, 20 mil Copper wire, annealed CFW-100-156 Lot #25477. ^{60}Co: <0.28 mBq/kg	Ge	<180	<86	101 ± 35
99	California Fine Wire, 20 mil annealed Cu wire, CFW-100-156, Lot #25477	Shiva Inc., GD-MS	<0.5	<10	<10
100	California Fine Wire, 20 mil annealed Cu–Be wire, alloy 25, CFW-100-034	Shiva Inc., GD-MS	<0.5	370 000	1 800 000
	Photo-etching: Cu on polyimide substrate				
101	Cu coating Nippon Steel Chemical Co., Espanex flat cable MC18-50-00CEM. Polyimide thickness: 50 μm, Cu thickness: 18 μm	ICP-MS	–	<3 (<0.05 pg/cm^2)	19 ± 2 (0.30 ± 0.03 pg/cm^2)
102	Polyimide substrate Nippon Steel Chemical Co., Espanex flat cable MC18-25-00 CEM, lot 65605-11R1. Polyimide thickness: 25 μm, Cu thickness: 18 μm	NAA[a]	<299	<1600	<1500

103	Cu coating Nippon Steel Chemical Co., Espanex flat cable MC18-25-00 CEM, lot 65605-11R1	ICP-MS	–	69 ± 3 (1.1 ± 0.05 pg/cm^2)	100 ± 3 (1.6 ± 0.04 pg/cm^2)
104	Polyimide substrate, Nippon Steel Chemical Co., Espanex flat cable, MC15-40-00 VEG. Polyimide thickness: 40 μm, Cu thickness: 15 μm	NAA[a]	107 ± 12	<450	<900
105	Cu coating, Nippon Steel Chemical Co., Espanex flat cable MC15-40-00 VEG	ICP-MS	–	135 ± 6 (1.8 ± 0.07 pg/cm^2)	67 ± 5 (0.9 ± 0.06 pg/cm^2)
106	Nippon Steel Chemical Co., Espanex flat cable MC15-40-00VEG. ^{60}Co: <0.18 mBq/kg	Ge	880 ± 120	<250	121 ± 32
107	Nippon Steel Chemical Co., Espanex flat cable MC18-25-00CEM, lot G5L03-23L2. ^{60}Co: <0.6 mBq/kg, ^{137}Cs: <1.3 mBq/kg	Ge	<146	<260	<46
108	Polyimide substrate, Nippon Steel Chemical Co., Espanex flat cable MC18-25-00CEM, lot G5C03 23L2	ICP-MS	390 ± 110 (1.4 ± 0.4 ng/cm^2)	50 ± 17 (0.54 ± 0.06 pg/cm^2)	450 ± 170 (1.6 ± 0.6 pg/cm^2)
109	Cu coating, Nippon Steel Chemical Co., Espanex flat cable MC18-25-00CEM, lot G5C03 23L2	ICP-MS	94 ± 19 (1.5 ± 0.3 ng/cm^2)	34 ± 6 (0.55 ± 0.09 pg/cm^2)	41 ± 6 (0.66 ± 0.1 pg/cm^2)
110	Nippon Steel, Espanex flat cable, MC15-40-00 VEG. Etched by Basic Electronics. ^{60}Co: <0.56 mBq/kg, ^{137}Cs: <0.63 mBq/kg	Ge	<160	<40	<97
111	Polyimide substrate Nippon Steel Espanex flat cable MC15-40-00 VEG. Etched Basic by Electronics	ICP-MS	229 ± 71 (1.3 ± 0.4 ng/cm^2)	317 ± 4 (1.8 ± 0.02 pg/cm^2)	3880 ± 120 (22 ± 0.7 pg/cm^2)
112	Cu coating Nippon Steel Espanex flat cable, MC15-40-00 VEG. Etched by Basic Electronics	ICP-MS	105 ± 23 (1.4 ± 0.3 ng/cm^2)	45 ± 4 (0.6 ± 0.05 pg/cm^2)	1720 ± 23 (23 ± 0.3 pg/cm^2)
	Avalanche photo diodes (including contact metals)				
113	White sand used by Advanced Photonix for die cutting or beveling APDs[b]	A.G. Ge	<38	$58\,000 \pm 4500$	$45\,300 \pm 1800$
114	Brown sand used for die cutting or beveling APDs	A.G. Ge	$720\,000 \pm 190\,000$	$(5.88 \pm 0.08) \times 10^7$	$(1.38 \pm 0.02) \times 10^7$
115	Hydro Aluminium Deutschland, GmbH 6N Al for APD fabrication, ID B06HP054	ICP-MS	170 ± 40	45 ± 2	44 ± 2
116	Pechiney Al for APDs. Extended cleaning	NAA	<460	<195	<560
117	Pechiney Al for APDs. Extended cleaning	ICP-MS	170 ± 60	33 ± 2	49 ± 2
118	Pechiney Al for APDs. Production cleaning only	ICP-MS	190 ± 40	38 ± 6	76 ± 4
119	Pechiney Al for APDs contact, no batch ID available	GD-MS	<100	<50	<50
120	Pechiney Al forAPDs	Ge	490 ± 160	<630	<360
121	Materials Research Corporation (MRC) Al for APDs, 20-101E-AL000-1000, purity grade 99.9995%	GD-MS	<50	42 000	6000
122	MRC Al for APDs 20-101E-AL000-1000, purity grade 99.9995%	Shiva Inc., GD-MS	<5	29 000	4100
123	MRC Al for APDs 20-101E-AL000-1000, purity grade 99.9995%	NAA	$<68\,000$	$48\,000 \pm 4800$	5500 ± 580
124	Ti for APD metallization	GD-MS	<200	<100	<100

Table 3 (*continued*)

#	Material	Method	K conc. (10^{-9} g/g)	Th conc. (10^{-12} g/g)	U conc. (10^{-12} g/g)
125	Pt for APD metallization	ICP-MS	–	32 ± 2	241 ± 4
126	Au for APD metallization	ICP-MS	–	612 ± 18	79 ± 2
127	Acid dissolved metal coating of Au contacted APD	ICP-MS	–	6200 ± 560	4500 ± 280
128	APD pre-production ring wafer, supplier B. Orientation 1,1,1. Production cleaning only	NAA[a]	<0.9	98 ± 10	13.9 ± 2.5
129	APD ring wafer, supplier A	NAA	3.6 ± 1	<1.8	<3.3
130	APD epi wafer	NAA	<7.9	<4.9	<4.9
131	APD with Al contact. SN:155-B489 Al. Made using MRC Al	NAA	30 ± 6	70 ± 8	<38
132	APD with Al contact. SN: 155-10-019 Al. Made using MRC Al	NAA	22 ± 4	101 ± 11	<24
133	APD with Au contact, made using MRC Al	NAA		<560	
134	APD with Au contact, madeusing MRC Al	Alpha counting[c]	–	<220	<73
	Heat transfer fluids and related hardware				
135	Cryogenic fluid 3M HFE-7000, lot 20016	NAA[a]	<1.08	<7.3	<6.2
136	Cryogenic fluid 3M HFE-7000, lot: 20016, after exposing to Wessington dewar	NAA[a]	<1.78	<2.8	<3.3
137	Cryogenic fluid 3M HFE-7000 lot 20018	NAA[a]	<0.59	<8.4	<3.4
138	Cryogenic fluid 3M HFE-7000, lot 920001	NAA	<0.58	<3.7	<7.3
139	Cryogenic fluid 3M HFE-7000, lot 20014. See Section 6 for analysis assumptions	Concentration+ NAA[a]	–	<0.015	<0.015
140	Cryogenic fluid 3M FC-87	NAA	<0.11	<0.95	<2.7
141	Cryogenic fluid 3M HFE-7100	NAA	<0.21	<1.2	<2.1
142	Cryogenic fluid 3M HFE-7100	NAA	<0.27	<3.4	<1.6
143	Silicon carbide. HFE pump thrust bearing material	A.G. Ge	$<65\,000$	$139\,000 \pm 39\,000$	$<44\,000$
144	Tungsten carbide. HFEpump shaft material	A.G. Ge	$<42\,000$	$<42\,000$	$<20\,000$
	Miscellaneous items				
145	JL Goslar Pb free soldering wire, Esold EN ISO 12224-1/SN99, 3CuO, 7/1.1, type B1	ICP-MS	–	<1	6570 ± 280
146	Fluka p-terphenyl 99% purity	NAA	72 ± 7	25 ± 3	0.5 ± 0.6
147	Macor insulators	A.G. Ge	$<680\,000$	$359\,000 \pm 41\,000$	$528\,000 \pm 4000$
148	Dow Corning ultra high vacuum grease	A.G. Ge	$<323\,000$	$<349\,000$	$116\,000 \pm 28\,000$
149	Translucent platinum-cured silicone rubber o-rings from Simolex. Compound #: SIM4768Pt, supplier #: 4105/60 (Elastosil)	Balazs Analytical Services, ICP-MS	640(sample A) and 950(sample B)	$<10\,000$	$<10\,000$
150	Transparent silicone-rubber o-rings from Perlast. Trans vmq 70-80 Plat Cured FDA/ WRCC/USP class 6 grade, Compound # S80U, batch P6976	Balazs Analytical Services, ICP-MS	790	$<10\,000$	$<10\,000$
151	Transparent silicone-rubber o-rings from Perlast. Trans vmq 70-80 Plat Cured FDA/ WRCC/USP class 6 grade, Compound No. S80U, batch P6820	Balazs Analytical Services, ICP-MS	1900	$<10\,000$	$<10\,000$

152	Transparent silicone-rubber o-rings from Perlast. Trans vmq 70-80 Plat Cured FDA/ WRCC/USP class 6 grade, Compound No. S80U, batch P6820	Ge	$<19\,200$	$<47\,000$	<7700
153	80 Buna-N Grotenrath Rubber Products Inc. o-rings of different sizes. Factor of 5 systematic uncertainty	A.G. Ge	26 ± 3.5	$23\,400 \pm 1200$	$21\,700 \pm 340$
154	Viton O-ring seal, Johannsen AG. ^{60}Co: <4.2 mBq/kg	Ge	$70\,000 \pm 7300$	32 000–54 000	$70\,000 \pm 7000$
155	Sapphire window from Swiss Jewel Company, substrate for EXO high voltage resistors. EXO sapphire lot 2	NAA[a]	<6.8	30 ± 7	<25
156	Sapphire window from Swiss Jewel Company, substrate for EXO high voltage resistors. EXO sapphire lot 1	Shiva Inc., GD-MS	<500	$<10\,000$	$<10\,000$
157	DuPont resistor paste 1108	Ge	5400 ± 1300	<4200	$11\,500 \pm 1800$
158	DuPont 6160 conductive paste	Ge	$43\,300 \pm 5700$	<7500	5240 ± 770
159	Resistive and conductive coating dissolved off EXO-200 sapphire-based field shaping resistors	ICP-MS	<820	<3000	<2500
160	Un-encapsulated electro-optical level sensors, Gems Sensors, Series ELS-900, P/N 2007200	Ge	$101\,000 \pm 14\,000$	$335\,000 \pm 66\,000$	$153\,000 \pm 21\,000$
161	Encapsulated electro-optical level sensors, Gems Sensors, Series ELS-900, P/N 2007200	Ge	$34\,000 \pm 3400$	$80\,000 \pm 16\,000$	$22\,000 \pm 3400$
162	Si screw, Si: WackerChemie, machining: Holm Siliciumbearbeitung	NAA	1.7 ± 0.3	<1.2	<1.0
163	TSMC 0.25 μm process IC chip	NAA	400 ± 300	<151	<3200
164	CuSn6 phosphor–bronze 6%. 3/4 hard, 0.8 mm thick	ICP-MS	<60	40 ± 4	88 ± 4
165	CuSn6 phosphor–bronze 6%. 3/4 hard, 0.8 mm thick. ^{60}Co: <0.60 mBq/kg, ^{137}Cs: 4.38 ± 0.53 mBq/kg	Ge	<360	<77	<170
166	CuSn6 phosphor–bronze 6%. 1/2 hard, 0.8 mm thick for cryostat door seal	ICP-MS	110 ± 40	50 ± 3	78 ± 4
167	CuSn6 phosphor–bronze 6%. 1/2 hard, 0.8 mm thick. ^{60}Co: <0.4 mBq/kg, ^{137}Cs: <1.6 mBq/kg	Ge	<320	<81	<136
168	1/2 in. 544 phosphor–bronze rod	ICP-MS	<20	15.9 ± 2.6	18.6 ± 2.3
169	1/4 in. phosphor–bronze washer. McMaster Carr #93490A029	ICP-MS	–	36 ± 4	43 ± 9
170	1/4 in. 20×1 in. phosphor–bronze bolt. McMaster Carr #93516A542	ICP-MS	188 ± 13	38 ± 4	43 ± 3
171	Belleville washers, phosphor–bronze, SOLON 8L80 PB. ^{60}Co: <0.55 mBq/kg	Ge	<280	1580 ± 260	1240 ± 140
172	Phosphor–bronze 544 for springs	Shiva Inc. GD-MS	<10	60	40
173	Silicon–bronze 651 for springs	Shiva Inc. GD-MS	<10	<5	<5
174	1/4 in. 655 silicon–bronze rod from Sequoia Brass and Copper	ICP-MS	–	6.2 ± 1.7	24.7 ± 3.2
175	1/4 in. rod of 655 silicon–bronze from National Bronze and Metals Inc	ICP-MS	97 ± 11	<4.7	<3.1

Table 3 (*continued*)

#	Material	Method	K conc. (10^{-9} g/g)	Th conc. (10^{-12} g/g)	U conc. (10^{-12} g/g)
176	1/4 in.-20 × 3/4 in. silicon–bronze screws. McMaster Carr #93516A540	ICP-MS	182 ± 15	<3.6	<3.9
177	1/2 in. silicon–bronze lock washer. McMaster Carr #93496A433	ICP-MS	139 ± 14	7.7 ± 2.4	<4.2
178	5/8 in.-11 × 2 in. silicon–bronze screws. McMaster Carr #93516A752	ICP-MS	<50	72 ± 8	83 ± 6
179	5/8 in. silicon–bronze lock washer. McMaster Carr #93496A435	ICP-MS	<60	24 ± 2	30 ± 3
180	5/8 in. silicon–bronze washer. McMaster Carr #93490A035	ICP-MS	<60	50 ± 4	43 ± 5
181	1/2 in.-13 × 2 in. hex head screws, C65100 Si-bronze. ^{60}Co: <0.46 mBq/kg	Ge	<620	<490	213 ± 51
182	Silicon–bronze screws and washers. ^{60}Co: <0.62 mBq/kg, ^{137}Cs: <0.70 mBq/kg	Ge	<250	<880	<120
183	Cu plus PET washers. ^{137}Cs: <10.7 ± 1.8 mBq/kg	Ge	<1040	<2800	2400 ± 350
184	Swagelok 1 in. copper gasket CU-1-16-RP-2	ICP-MS	229 ± 16	9.1 ± 1.7	20.4 ± 2.5
185	Swagelok 1 in. brass fitting 1610-1-16RS	ICP-MS	<19	8.2 ± 2	27.4 ± 2.4
186	Swagelok 1/2 in. brass fitting B-810-1-12, machined to custom shape	ICP-MS	–	12.5 ± 1.4	12.4 ± 1.3
187	Swagelok 1/2 in. brass fitting B-810-1-12, extra cleaning, machined to custom shape	ICP-MS	–	5.1 ± 0.7	7.9 ± 0.7
188	Swagelok ferrules for brass fitting B-810-1-12, second shipment. Machined to custom shape	ICP-MS	<28	12 ± 1	10.0 ± 0.8
189	Swagelok body for brass fitting B-810-1-12, second shipment. Machined to custom shape	ICP-MS	<35	<2.7	<1.7
190	1/2 in. copper gasket, Serto #SO 40007-18	ICP-MS	260 ± 31	6.9 ± 2.5	12.6 ± 2.2
191	1/2 in. copper gasket, Serto #SO 40007-18. Second shipment	ICP-MS	–	7.5 ± 3.5	10.2 ± 2.8
192	1/2 in. Indium plated (New Brunswick Plating) Serto copper gasket. Un-plated gasket is item 190	ICP-MS	189 ± 22	7.5 ± 1.3	19.2 ± 2.4
193	Indium plated (New Brunswick Plating) Jetseal phosphor–bronze gasket. phosphor–bronze is item 166	ICP-MS	–	66.9 ± 6.0	78.2 ± 9.7
194	1 in. Indium plated (New Brunswick Plating) copper gasket. Un-plated gasket is item 184	ICP-MS	146 ± 14	14.5 ± 1.5	27.5 ± 3.1
195	Helicoil Stainless Steel, various sizes (194 × 1/2-13 1185-8CN500 190 × 1/4-20 1185-4CN375 96 × 3/4-20 1185-12CN750 190 × 8-32 1185-2CN328). ^{60}Co: 41 ± 2 mBq/kg	Ge	<430	<320	<193
196	10 gauge copper wire, MacMaster-Carr, ID 7512 K552. ^{60}Co: <0.23 mBq/kg, ^{137}Cs: <1.5 mBq/kg	Ge	1190 ± 250	<77	<270

197	10 gauge copper wire, MacMaster-Carr, ID 7512 K552	ICP-MS	–	30 ± 2	11 ± 1
198	10 gauge copper wire, MacMaster-Carr, ID 7512 K552. Second purchase	ICP-MS	<60	29 ± 2	16 ± 1
199	Polyethylene insulator from Consolidated Wire and Cable RG217 coax high voltage cable	NAA	47 ± 7	<140	<240
200	Copper wire from Consolidated Wire and Cable RG217 coax high voltage cable	ICP-MS	118 ± 17	4.4 ± 2.6	6.0 ± 2.5
201	Polyethylene insulator from Pasternack RG217 coax high voltage cable	NAA	129 ± 17	<360	355 ± 107
202	Copper wire from Pasternack RG217 coax high voltage cable	ICP-MS	105 ± 15	<4.7	4.1 ± 2.3
203	20 gauge silicone rubber high voltage cable from Able Wire Company. ^{60}Co: <0.62 mBq/kg, ^{137}Cs: <0.71 mBq/kg	Ge	$19\,200 \pm 2100$	$36\,400 \pm 3700$	$34\,600 \pm 3500$
204	Two component urethane potting mixture, Epoxies Etc. Resin 20-2350R CLR, catalyst 20-2350C, 100:7.5 mix	NAA[a]	11.4 ± 2.2	<37	<94
205	Two component epoxy, Epoxies Etc. Resin 20-3001R clear, catalyst 20-3001C, 1:1 mix	NAA[a]	<20	<23	<44
206	Two component low temperature silicone rubber. Component A GE-RTV567A product# 009454, component B GE-RTV567B, product# 38014, 15:1 mix	NAA[a]	$(14.4 \pm 1.4) \times 10^6$	–	237 ± 59
207	Epon 828 epoxy resin, manufactured by Hexion. ^{60}Co: <0.5 mBq/kg, ^{137}Cs: <0.5 mBq/kg	Ge	<200	<150	<250
208	14 m 1/4 in. OD, 1/6 in. ID PTFE tubing, MacMaster-Carr # 5033 K316. ^{60}Co: <5.8 mBq/kg, ^{137}Cs: <10.8 mBq/kg	Ge	<6400	<700	<2900
209	3/16 in. Copper tubing. Wolverine Tube Inc. McMaster Carr # 5174 K2, Cu alloy 122	ICP-MS	<60	74 ± 4	<1
210	1/2 in. Cu tubing for heat exchangers. Metallica SA	ICP-MS	–	<2	<1.5
211	1/2 in. Cu tubing for heat exchangers. Metallica SA	Ge	<180	<790	<113
212	1 in. Cu tubing for HFE. McMaster-Carr, Cu-alloy 122	ICP-MS	<27	40 ± 2	<1.5
213	Closed cell PE foam, Uline 1/8 in. × 72 in. × 550'. ^{60}Co: <23 mBq/kg, ^{137}Cs: <29 mBq/kg	Ge	$<14\,800$	$<19\,200$	$32\,000 \pm 4600$
214	Closed cell PE foam, Pacific States Felt & Mfg. co. Inc., 1/8 in. thick	NAA[a]	7820 ± 960	14000 ± 4000	<4900
215	Omega Engineering Inc. thermocouple, part TT-T-30-SL. ^{60}Co: <8.0 mBq/kg	Ge	<7000	<3800	<1700
216	Polyimide tape from Stanford stock room	A.G. Ge	$<37\,000$	<5400	<5800
217	Sheldal superinsulation, item # 146477, 0.25 mil PET aluminized on one side	Ge	5550 ± 1300 (4.9 ± 1.2 ng/cm^2)	<4080 (<3.7 pg/cm^2)	4660 ± 380 (4.1 ± 0.4 pg/cm^2)

Table 3 (*continued*)

#	Material	Method	K conc. (10^{-9} g/g)	Th conc. (10^{-12} g/g)	U conc. (10^{-12} g/g)
218	Sheldal superinsulation, item # 146477, 0.25 mil PET aluminized on one side. K result is for dissolved aluminum layer only but normalized to whole sample mass. For U and Th, the PET layer was also partially dissolved and analyzed	ICP-MS	461 ± 33 (0.41 ± 0.03 ng/cm^2)	<1800 (<1.6 pg/cm^2)	5740 ± 150 (5.1 ± 1.3 pg/cm^2)
219	Sheldal superinsulation, item # 146455, 0.3 mil DuPont Kapton aluminized on one side	ICP-MS	–	<1640 (<1.75 pg/cm^2)	<6100 (<6.5 pg/cm^2)
220	Sheldal superinsulation, item # 146428, 0.3 mil DuPont Kapton aluminized on both sides, embossed	ICP-MS	–	<1540 (<1.64 pg/cm^2)	2500 ± 800 (2.64 ± 0.85 pg/cm^2)
221	Jehier candidate superinsulation mix for EXO before installation: 26 layers of Insulray 305 plus four layers of Teril-53. ^{60}Co: <3.8 mBq/kg	Ge	<6500	<4100	7700 ± 1000
222	Jehier superinsulation mix sampled after installation without further cleaning	NAA	$51\,400 \pm 2100$	$<13\,900$	$12\,300 \pm 5540$
223	Plastic and metallization of Jehier superinsulation EXO-mix	ICP-MS	–	<80	<60
224	Jehier superinsulation, EXO-mix. Second purchase. ^{60}Co: <16 mBq/kg, ^{137}Cs: <16 mBq/kg	Ge	$18\,600 \pm 5000$	<1700	3900 ± 1300
225	Jehier hook-and-loop fastener to hold superinsulation	Ge	3090 ± 890	<1670	<920

Manufacturer production lot numbers or arbitrary identifiers are indicated for materials where multiple lots were studied. Uncertainties are quoted at 68% C.L. and limits are 95% C.L. Results which are less than 3-σ above zero (not including systematic scaling uncertainties) are reported as upper limits. GD-MS measurements have a factor of two uncertainty. In the "method" column, "A.G. Ge" refers to above ground germanium counting. Measurements with methods of "Balazs Analytical Services" or "Shiva Inc." were performed by the commercial services of the respective companies. Entries 31 and 38 list data taken from Refs. [18] and [19], respectively, as indicated. Where available, germanium counting results for ^{60}Co and ^{137}Cs activities are given within the sample descriptions.

[a]Indicated NAA results may be affected by a neutron flux calibration discrepancy described in Section 5. The tabulated results do not include systematic uncertainties arising from this discrepancy.

[b]All APDs listed in this table were produced by Advanced Photonix, Inc.

[c]APD alpha counting was performed using the APD as both the sample and the detector, and is only sensitive to alphas from the active volume of the APD.

roughly 20% measurement uncertainty. A few batches varied by as much as 50%, and ultimately three batches were thus rejected before homogenization. In Table 2 we report the analysis results of levels of ^{210}Pb in the EXO-200 lead as well as other lead varieties studied. Alpha spectra from lead samples are shown in Fig. 6 along with a background spectrum.

All candidate Doe Run batches and all homogenized batches were tested for K, Th, and U levels using GD-MS analysis. Selected batches, including all of the homogenized batches, were further tested using ICP-MS, which provided higher sensitivity to the uranium and thorium content. All three homogenized batches were found to have levels of K less than 7×10^{-9} g/g and both Th and U levels below $<1 \times 10^{-12}$ g/g. However, a few of the original candidate Doe Run batches did show levels higher than these limits. Some of these were rejected for use in forming the EXO lead.

8. Summary

Previous attempts to reduce intrinsic radioactive backgrounds in detector systems have generally focused on studies of a few common primary construction materials such as copper and lead. In order to facilitate development of complex low-background detector systems, clean materials must be available for producing a wide variety of parts. We have performed a systematic study of trace radioactive impurities in a large variety of parts and materials, focusing on those required to construct the EXO-200 cryogenic TPC detector system (See Table 3). As well as finding suitable raw materials and commercially available parts, we have also shown quantitatively that efforts to improve cleanliness of the production and handling of parts can result in measurable improvements in radiopurity. We hope that these studies will help to facilitate the advancement and development of the next generation of low-background counting facilities, both by helping to reduce background levels below what has previously been achieved, and by allowing the construction of more complex purpose-built detection systems.

Acknowledgments

We thank Dirk Arnold at PTB for contributed data, Kenji Kingsford at Saint Gobain for extensive help with Teflon selection and finishing, as well as Niel Washburn, Richard Van Ryper, and Sharon Libert at DuPont for consultations and generous materials donations. We thank Edward Lau, Susan Tucker and Judith Maro at MITR as well as David Woisard, APT, API, and Vaga Industries for their accommodating cooperation. This work was supported in part by the US Department of Energy under contract number DE-FG02-01ER4166.

References

[1] M. Danilov, et al., Phys. Lett. B 480 (2000) 12;
M. Breidenbach, et al., Letter of intent to SLAC EPAC, LOI–2001.1, August 2001, unpublished.
[2] F. LePort, A. Pocar, et al., Nucl. Instr. and Meth. A 578 (2007) 407.
[3] M. Redshaw, et al., Phys. Rev. Lett. 98 (2007) 053003.
[4] E.-I. Esch, et al., Nucl. Instr. and Meth. A 538 (2005) 516.
[5] C.L. Chou, J.D. Moffatt, Fresenius J. Anal. Chem. 368 (2000) 59.
[6] A.E. Eroglu, C.W. McLeod, K.S. Leonard, D. McCubbin, Spectrochim. Acta Part B At. Spectrosc. 53 (1998) 1221.
[7] J.C. Lozano, F. Fernandez, J.M.G. Gomez, Appl. Radiat. Isot. 50 (1999) 475.
[8] J.S. Becker, H.J. Dietze, J. Anal. At. Spectrom. 13 (1998) 1057.
[9] J.S. Becker, W. Kerl, H.J. Dietze, Anal. Chim. Acta 387 (1999) 145.
[10] K. Tagami, S. Uchida, J. Radioanal. Nucl. Chem. 197 (1995) 409.
[11] S. Vijayalakshmi, R.K. Prabhu, T.R. Mahalingam, C.K. Mathews, At. Spectrosc. 13 (1992) 61.
[12] H.E. Carter, P. Warwick, J. Cobb, G. Longworth, Analyst 124 (1999) 271.
[13] J. Chai, Y. Oura, M. Ebihara, J. Radioanal. Nucl. Chem. 255 (2003) 471.
[14] A.P. Mykytiuk, P. Semeniuk, S. Berman, Spectrochim. Acta Rev. 13 (1990) 1.
[15] M.R. Winchester, R. Payling, Spectrochim. Acta Part B At. Spectrosc. 59 (2004) 607.
[16] P. Grinberg, S. Willie, R.E. Sturgeon, Anal. Chem. 77 (2005) 2432.
[17] Z. Djurcic, D. Glasgow, L.-W. Hu, R. McKeown, A. Piepke, R. Swinney, B. Tipton, Nucl. Instr. and Meth. A 507 (2003) 680.
[18] D. Arnold, Private communication, 2003.
[19] J. Boger, et al., Nucl. Instr. and Meth. A 449 (2000) 172.